J|A|C|S COMMUNICATIONS

Published on Web 03/24/2010

Thermally Stable Pt/CeO_2 Hetero-Nanocomposites with High Catalytic Activity

Huan-Ping Zhou, Hao-Shuai Wu, Jie Shen, An-Xiang Yin, Ling-Dong Sun, and Chun-Hua Yan*

Beijing National Laboratory for Molecular Sciences, State Key Laboratory of Rare Earth Materials Chemistry and Applications & PKU-HKU Joint Laboratory in Rare Earth Materials and Bioinorganic Chemistry, College of Chemistry and Molecular Engineering, Peking University, Beijing 100871, China

Received February 7, 2010; E-mail: yan@pku.edu.cn

Model nanocatalysts with tunable size, shape, and composition drew tremendous interest in both theoretical and technological fields in recent years, since they are promising materials for unveiling the interrelation between catalytic activity or selectivity and the characteristics of catalysts.[1] By virtue of their narrow size distribution, fine dispersibility in various media, tunable shapes and sizes, and accessibility for the construction of hetero-nanocomposites, colloidal nanoparticles have been proven to be ideal model nanocatalysts.[2] However, as these materials are relatively unstable and tend to agglomerate during high temperature reactions, it is of vital importance to enhance their thermal and chemical stability without impairing their intrinsic high performance.[3]

As a most important functional rare earth oxide, ceria-based materials are attractive with extensive applications in conversion catalysts, three-way catalysts (TWCs), fuel cells, solar cells, gates for metal oxide semiconductor devices, and phosphors.[4] Many studies on ceria-based materials toward exhaust emission have demonstrated that the capacity for rapid storage and release of oxygen at their surface is mainly associated with the ceria−noble metal interaction.[5] To promote CO oxidation and a water-gas shift reaction, particularly at the early stage of an engine start, the construction of noble metal/CeO_2 nanocomposites with high thermal stability and catalytic activity becomes a great challenge.

In this Communication, we report a facile method to synthesize uniform Pt/CeO_2 hetero-nanocomposites. The procedures (Scheme 1) include the microemulsion-mediated synthesis of $Pt/CeO_2@SiO_2$, the calcination of $Pt/CeO_2@SiO_2$, and the removal of a SiO_2 shell.[6a] In a typical synthesis, the cyclohexane solution, polyoxyethyleneonyl pheny ether (Igepal CO-520), and aqueous solution formed a microemulsion system, in which the hydrophobic ceria nanoparticles (Figure S1 in Supporting Information (SI)) and Pt precursors could be blended evenly in the microemulsion droplets.[6] After the subsequent addition of NH_4OH aqueous solution and tetraethyl orthosilicate (TEOS), uniform $Pt/CeO_2@SiO_2$ with maximized Pt/CeO_2 interfaces was obtained. In addition, the SiO_2 shells separate the inner nanocomposites and thus prevent their aggregation during calcination. As a result, after removal of the SiO_2 shells, these hetero-nanocomposites exhibit high thermal stability and improved catalytic activity compared with the mixture of Pt and CeO_2 in the CO oxidation reaction.

Transmission electron microscopy (TEM) analyses show the formation of monodisperse $Pt/CeO_2@SiO_2$ (Figure 1a). After calcination in air at 450 °C, the crystallinities of both Pt and CeO_2 nanoparticles in these composites are improved, while their morphologies are well maintained. These are confirmed by a TEM image (Figure 1b), in which nearly each SiO_2 sphere contains one CeO_2 nanocrystal and several surrounding Pt nanoparticles. The CeO_2 and Pt nanocrystals are cubic and truncated octahedral in shape, with average sizes of 5−6 nm and 1−2 nm, respectively. As shown in the inset of Figure 1b, a high-resolution TEM

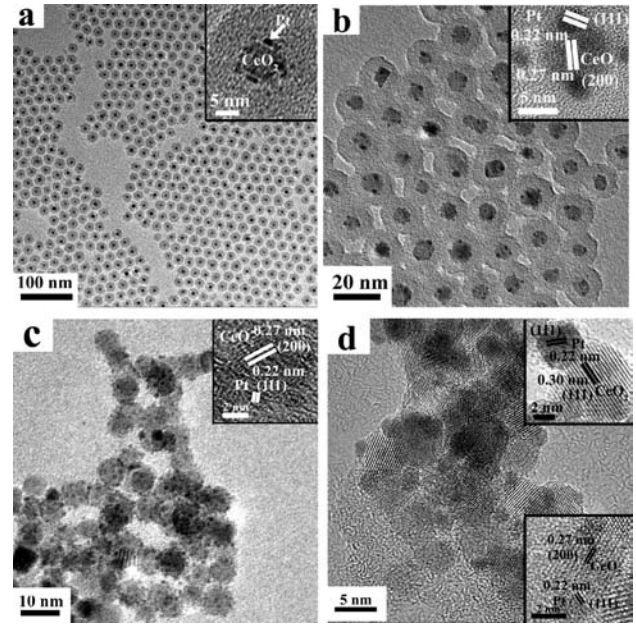

Figure 1. TEM images and HRTEM images (inset) of the samples: (a) as-prepared $Pt/CeO_2@SiO_2$; (b) calcined $Pt/CeO_2@SiO_2$; (c) Pt/CeO_2 hetero-nanocomposites; (d) calcined Pt/CeO_2 hetero-nanocomposites.

(HRTEM) image of the nanocomposite indicates that the CeO_2 nanocrystal is enclosed by {100} facets, as can be confirmed from the lattice fringes with an interplanar distance of 0.27 nm, while the surrounding Pt particles are enclosed by the {111} facets, according to the existing 0.22 nm interplanar distance. The spectrum of energy-dispersive X-ray analysis (EDAX) (Figure S2 in SI) confirms its homogeneous composition, and the Pt/Ce ratio is 1:3, according to the inductively coupled plasma mass spectrometry measurement result. In addition, $Pt/CeO_2@SiO_2$ with different Pt/Ce ratios (Figure S3 in SI) can be obtained, while these structures are stable up to 800 °C (Figure S4 in SI).

The SiO_2 shells of the Pt/CeO_2 hetero-nanocomposites are dissolved by aqueous NaOH solution after sintering. Figure 1c and Figure S5 in SI shows the TEM images of the as-obtained Pt/CeO_2 hetero-nanocomposites, revealing the maintenance of the crystallinity and morphologies of the core composites after the removal of the SiO_2 matrix. The HRTEM image shown in the inset of Figure 1c demonstrates that the resultant composites of Pt/CeO_2 are of low aggregation and indeed consist of a single CeO_2 nanocrystal and surrounding Pt nanocrystals. More importantly, when the as-obtained Pt/CeO_2 hetero-nanocomposites are calcined at 450 °C, as shown in Figure 1d, the products still inherit their original morphology basically, without a significant increase in the nanocrystal size and loss of the CeO_2 and Pt interfaces. Generally, when calcined at high temperature, small nanoparticles are more liable

10.1021/ja101110m

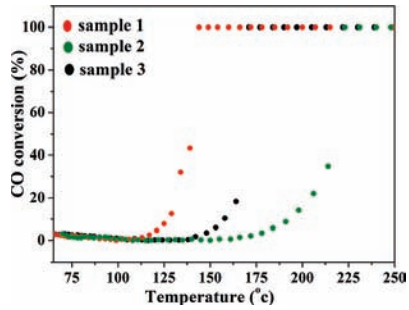

Figure 2. CO conversion vs reaction temperature over the catalysts of Pt/CeO_2 hetero-nanocomposites and two kinds of mixture of CeO_2 and Pt.

to aggregate, coalesce, and grow to minimize the surface energy. Herein, we believe that the good durability against heat treatment of the present Pt/CeO_2, which can keep their pristine properties even after the calcination at 450 °C, originates probably from the earlier calcination treatment of $Pt/CeO_2@SiO_2$. In this process, the SiO_2 shells hinder further mergence and growth of the CeO_2 and Pt nanoparticles at high temperature, and accordingly, under the protection of a silica shell, these nanoparticles are capable of maintaining their initial nanostructures while improving crystallinity concurrently. Thus, Pt/CeO_2, with a relatively small particle size, maximized Pt/CeO_2 interfaces, and especially sufficient thermal stability (Figure S6 in SI), may serve as an excellent catalytic model for important high-temperature catalytic reactions.

In the fields of exhaust emission control and fuel cells, the composite of ceria and noble metal is one of the most prevalent systems to explore the catalytic oxidation of CO to CO_2. Here, the performance at high temperature of the Pt/CeO_2 was investigated using the CO oxidization as a model reaction. Three samples with the same Pt/Ce ratio were used. Sample 1 was obtained by calcination of the Pt/CeO_2 hetero-nanocomposites (Figure 1d). Sample 2 was obtained by respectively calcining Pt and CeO_2 nanoparticles and further mixing them together (Pt nanoparticles before and after calcination were shown in Figure S7a,b, and CeO_2 nanoparticles before and after calcination were shown in Figures S1 and S7c in SI). Sample 3 was obtained by respectively preparing $Pt@SiO_2$ and $CeO_2@SiO_2$ (Figure S7d,e in SI), further calcination and then removal of the silica shell, followed by a second calcination treatment (Figure S7f,g in SI), and mixing them together. Figure 2 shows the plot of CO conversion percentage versus reaction temperature for these three samples. For the CO conversion to CO_2 from 65 to 250 °C, the 100% conversion temperatures of the catalysts are found to follow the sequence of sample 1 (144 °C) < sample 3 (171 °C) < sample 2 (223 °C). The BET specific surface areas of the samples 1, 2, and 3 were determined to be 83, 70, and 76 $m^2\ g^{-1}$, respectively, which is consistent with the above activity sequence. However, the slight difference among these data does not seem sufficiently responsible for the major variation in catalytic performances. Thus, besides particle size, some other factors, such as particle dispersity, and the interaction of oxide and noble metal probably play important roles in the catalytic activity of nanocomposites.[7] According to the TEM images (Figures 1d and S7b,c in SI), it is obvious that, compared with sample 2, sample 1 exhibits a smaller particle size and lower aggregation between particles, which convincingly contribute to their lower 100% conversion temperature. However, although the particle size and aggregation degree for the samples 1 and 3 are similar, as shown by Figures 1d and S7f,g in SI, a notable difference is also observed in regard to their catalytic activity. This can be ascribed to the existence of more

Scheme 1. Synthesis Protocol of $Pt/CeO_2@SiO_2$ Nanospheres and Pt/CeO_2 Hetero-Nanocomposites

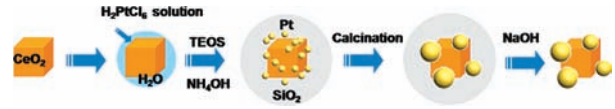

Pt/CeO_2 interfaces in sample 1, which have positive effects on the interaction of CeO_2 and Pt, and thus on the catalytic activity. Therefore, these results strongly suggest that the Pt/CeO_2 hetero-nanocomposites would have potential applications in various catalytic fields, especially in high-temperature catalytic reactions.

In conclusion, we demonstrate a facile method for the synthesis of Pt/CeO_2 hetero-nanocomposites from $Pt/CeO_2@SiO_2$. The final Pt/CeO_2 without silica encapsulation shows not only an enhanced catalytic activity (Figure S8 in SI) but also a good thermal stability. Compared with the mixture of Pt and CeO_2, this thermally stable Pt/CeO_2 nanocomposite exhibits the characteristics of small size as in the case of Pt and CeO_2, low aggregate of particles, and a large number of Pt and CeO_2 interfaces, assuring their high catalytic activity in CO oxidation. This approach is simple albeit efficient and can be potentially extended to the synthesis of other composites of noble metals and oxides. This work has opened a new window for the construction of hetero-nanocomposites with high activity and would serve as excellent model in high-temperature catalytic systems of both theoretical and practical interest.

Acknowledgment. We gratefully acknowledge the financial support from the MOST of China (Grant No. 2006CB601104) and NSFC (Grant Nos. 20821091 and 20871006).

Supporting Information Available: The synthesis details, more TEM images, EDAX, and catalytic results of the CeO_2, Pt, and CeO_2/$Pt@SiO_2$ nanoparticles. This material is available free of charge via the Internet at http://pubs.acs.org.

References

(1) (a) Song, H.; Rioux, R. M.; Hoefelmeyer, J. D.; Komor, R.; Niesz, K.; Grass, M.; Yang, P. D.; Somorjai, G. A. *J. Am. Chem. Soc.* **2006**, *128*, 3027. (b) Narayanan, R.; El-Sayed, M. A. *Nano Lett.* **2004**, *4*, 1343. (c) Tian, N.; Zou, Z. Y.; Sun, S. G.; Ding, Y.; Wang, Z. L. *Science* **2007**, *316*, 732. (d) Bratlie, K. M.; Lee, H.; Komvopoulos, K.; Yang, P. D.; Somorjai, G. A. *Nano Lett.* **2007**, *7*, 3097. (e) Alayoglu, S.; Nilekar, A. U.; Mavrikakis, M.; Eichhorn, B. *Nat. Mater.* **2008**, *7*, 333.

(2) (a) Park, J.; Joo, J.; Kwon, S. G.; Jang, Y.; Hyeon, T. *Angew. Chem., Int. Ed.* **2007**, *46*, 4630. (b) Ahmadi, T. S.; Wang, Z. L.; Green, T. C.; Henglein, A.; El-Sayed, M. A. *Science* **1996**, *272*, 1924. (c) Sun, Y.; Xia, Y. *Science* **2002**, *298*, 2176. (d) Wang, C.; Diamon, H.; Sun, S. H. *Nano Lett.* **2009**, *9*, 1493.

(3) (a) De Rogatis, L.; Cargnello, M.; Gombac, V.; Lorenzut, B.; Montini, T.; Fornasiero, P. *ChemSusChem* **2010**, *3*, 24. (b) Zhang, P.; Chi, M.; Sharmaa, S.; McFarland, E. *J. Mater. Chem.* **2010**, *20*, 2013.

(4) (a) Fu, Q.; Saltsburg, H.; Flytzani-Stephanopoulos, M. *Science* **2003**, *301*, 935. (b) Kašpar, J.; Fornasiero, P.; Graziani, M. *Catal. Today* **1999**, *50*, 285. (c) Murray, E. P.; Tsai, T.; Barnett, S. A. *Nature* **1999**, *400*, 649. (d) Corma, A.; Atienzar, P.; Garcia, H.; Chane-Ching, J. Y. *Nat. Mater.* **2004**, *3*, 394. (e) Tye, L.; El-Masry, N. A.; Chikyowm, T.; McLarty, P.; Bedair, S. M. *Appl. Phys. Lett.* **1994**, *65*, 3081. (f) Morshed, A. H.; Moussa, M. E.; Bedair, S. M.; Leonard, R.; Liu, S. X.; El-Masry, N. *Appl. Phys. Lett.* **1997**, *70*, 1647.

(5) (a) Bernal, S.; Kaspar, J.; Trovarelli, A. *Catal. Today* **1999**, *50*, 173. (b) Tibiletti, D.; Goguet, A.; Meunier, F. C.; Breen, J. P.; Burch, R. *Chem. Commun.* **2004**, 1636. (c) Yeung, C. M. Y.; Yu, K. M. K.; Fu, Q. J.; Thompsett, D.; Petch, M. I.; Tsang, S. C. *J. Am. Chem. Soc.* **2005**, *127*, 18010. (d) Yeung, C. M. Y.; Tsang, S. C. *J. Phys. Chem. C* **2009**, *113*, 6074. (e) Cargnello, M.; Wieder, N. L.; Montini, T.; Gorte, R. J.; Fornasiero, P. *J. Am. Chem. Soc.* **2010**, *132*, 1402.

(6) (a) Shin, J.; Kim, H.; Lee, I. S. *Chem. Commun.* **2008**, 5553. (b) Masih Darbandi, M.; Thomann, R.; Nann, T. *Chem. Mater.* **2005**, *17*, 5720.

(7) (a) Nikolaev, S. A.; Smirnov, V. V. *Catal. Today* **2009**, *147*, S336. (b) Zheng, Y. H.; Chen, C. Q.; Zhan, Y. Y.; Lin, X. Y.; Zheng, Q.; Wei, K. M.; Zhu, J. F. *J. Phys. Chem. C* **2008**, *112*, 10773. (c) Xu, L. S.; Ma, Y. S.; Zhang, Y. L.; Jiang, Z. Q.; Huang, W. X. *J. Am. Chem. Soc.* **2009**, *131*, 16366.

JA101110M